Cite this: *Soft Matter*, 2012, **8**, 6573

www.rsc.org/softmatter

PAPER

Surfactant adsorption and aggregate structure at silica nanoparticles: Effects of particle size and surface modification†

Bhuvnesh Bharti,[a] Jens Meissner,[a] Urs Gasser[b] and Gerhard H. Findenegg*[a]

Received 20th March 2012, Accepted 13th April 2012
DOI: 10.1039/c2sm25648g

The influence of particle size and a surface modifier on the self-assembly of the nonionic surfactant $C_{12}E_5$ at silica nanoparticles was studied by adsorption measurements and small-angle neutron scattering (SANS). Silica nanoparticles of diameter 13 to 43 nm were synthesized involving the basic amino acid lysine. A strong decrease of the limiting adsorption of $C_{12}E_5$ with decreasing particle diameter was found. To unveil the role of lysine as a surface modifier for the observed size dependence of surfactant adsorption, the morphology of the surfactant aggregates assembled on pure siliceous nanoparticles (Ludox-TMA, 27 nm) and their evolution with increasing lysine concentration at a fixed surfactant-to-silica ratio was studied by SANS. In the absence of lysine, the surfactant forms surface micelles at silica particles. As the concentration of lysine is increased, a gradual transition from the surface micelles to detached wormlike micelles in the bulk solution is observed. The changes in surfactant aggregate morphology cause pronounced changes of the system properties, as is demonstrated by turbidity measurements as a function of temperature. These findings are discussed in terms of particle surface curvature and surfactant binding strength, which present new insight into the delicate balance between the two properties.

1. Introduction

Surfactant adsorption onto colloidal particles is of eminent importance to technological processes in which colloidal stability or detergency plays a role.[1] Surfactant adsorption onto hydrophilic surfaces can be regarded as a surface aggregation process, reminiscent of micelle formation in solution.[2–9] When the anchoring of the surfactant heads to the surface is weak, as in the case of nonionic surfactants at oxide surfaces, the morphology of surface aggregates may depend both on the anchoring strength[10,11] and on the curvature of the adsorbing surface.[12–18] For instance, for the surfactant penta(ethyleneglycol) monododecylether ($C_{12}E_5$) it was recently found that discrete surface micelles are formed on silica nanoparticles,[14,16] although flat bilayer aggregates are preferred at planar silica surfaces.[6,7] At even weaker anchoring energies, surface micelles may be disfavoured against micelles in solution, implying that little or no adsorption occurs, as in the case of dodecyl maltoside (β-$C_{12}G_2$) at silica nanoparticles.[14]

Here, we study the influence of particle size and surface modification on the adsorption of the surfactant $C_{12}E_5$ at silica nanoparticles. The particles were synthesized by a modified Stöber method[19] yielding particles of narrow size distribution down to the 10 to 50 nm size range which was of interest in this study. In this method, the basic amino acid lysine is used instead of ammonia as the catalyst for the hydrolysis of the silica precursor. For the resulting Lys–Sil particles[19] it was found that the adsorption isotherm of $C_{12}E_5$ exhibits a pronounced dependence on particle size. To assess the influence of lysine on the surface energy and the adsorption of the surfactant at the silica particles we also investigated the adsorption of lysine onto pure siliceous silica nanoparticles (Ludox-TMA) and used small angle neutron scattering (SANS) to elucidate changes in surfactant self-assembly when adding increasing amounts of lysine to the silica dispersion. Based on these results we discuss the effects of surface curvature and anchoring strength of the surfactant heads on the adsorption of $C_{12}E_5$ at silica nanoparticles.

2. Results

2.1 Characterization of silica nanoparticles

Results of the characterization of three Lys–Sil materials by small-angle X-ray scattering (SAXS), nitrogen adsorption and TEM are shown in Fig. 1. The SAXS profiles of the three samples

[a]*Technische Universität Berlin, Institut für Chemie, Stranski Laboratorium, TC 7, Strasse des 17. Juni 124, D-10623 Berlin, Germany. E-mail: findenegg@chem.tu-berlin.de; Fax: +49 30 314 26602; Tel: +49 30 314 24171*

[b]*Paul Scherrer Institut, 5232 Villigen, Switzerland. E-mail: urs.gasser@psi.ch; Fax: +41 56 3102939; Tel: +41 56 3103229*

† Electronic supplementary information (ESI) available: Characterization of Ludox-TMA silica nanoparticles; analysis of SANS data; SAXS for temperature variation experiments. See DOI: 10.1039/c2sm25648g

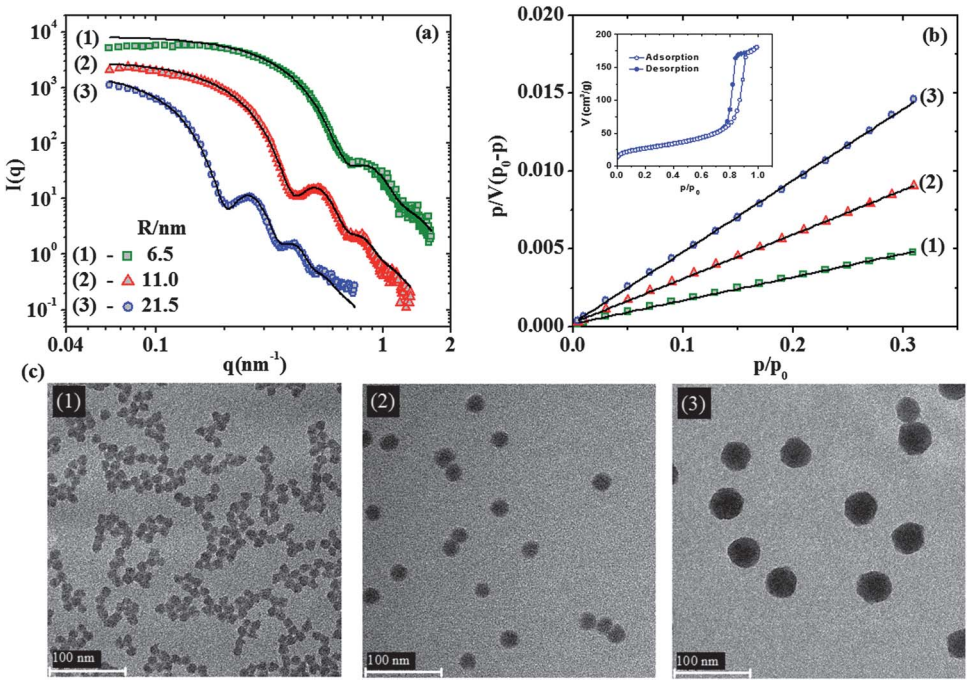

Fig. 1 Characterization of three Lys–Sil silica (1), (2) and (3): (a) experimental SAXS profiles and fits to the points according to form factor of spheres dispersed in a medium. (b) BET-plot of N_2 adsorption isotherms (the inset is the measured complete isotherm for Lys–Sil-3 silica particles). (c) TEM images of the three Lys–Sil nanoparticles, shown at the same magnification.

(Fig. 1a) can be represented by the form factor model of spherical particles having a log-normal size distribution. Values of the mean particle radius R and polydispersity s of the three Lys–Sil materials are given in Table 1. The systematic deviations from the experimental $I(q)$ at low values of the scattering vector q can be attributed to repulsive long-range interactions between the charged particles at pH 9. These interparticle features are of no relevance for the mean particle size and size distribution.

The specific surface area of the silica sols was determined from the nitrogen adsorption isotherms by the BET method in a range of relative pressures p/p_0 from 0.05 to 0.3 (Fig. 1b). The resulting values a_{BET} are given in Table 1 and compared with the geometric surface area per unit mass, $a_{geo} = 3/R\rho_{SiO2}$, with R the mean particle radius (from SAXS) and ρ_{SiO2} the density of silica (2.2 g cm^{-3}).

2.2 Surfactant adsorption onto Lys–Sil nanoparticles

Adsorption isotherms of the surfactant $C_{12}E_5$ at the three Lys–Sil sols at pH 7 and 20 °C are shown in Fig. 2. The graphs present the surface concentration Γ of the surfactant (amount adsorbed per unit area) *vs.* solution concentration expressed in the units of the critical micelle concentration (cmc = 7 × 10^{-5} M at 20 °C). The isotherms exhibit a steep increase in adsorption starting at an onset concentration below the cmc, and a plateau value that is reached shortly above the cmc. The isotherms can be represented by the S-type isotherm equation by Gu and Zhu,[20]

$$\Gamma = \Gamma_m \frac{K(c/\mathrm{cmc})^n}{1 + (c/\mathrm{cmc})^n} \quad (1)$$

where Γ_m represents the maximum surface concentration (plateau value of the adsorption isotherm), K is the adsorption constant and n is nominally the aggregation number of surface micelles. Fits of eqn (1) to the adsorption data are shown by the full curves in Fig. 2 and the parameters are summarized in Table 2. Also given is the surface aggregation concentration c_0, which can be calculated from the parameters K and n by eqn (2):[20]

Table 1 Parameters for synthesis and characterization of three Lys–Sil samples: stirring rate r of the reaction mixture at temperature T, mean particle radius R and size polydispersity s as derived from SAXS, and specific surface area a_{BET} of the sols as determined from the nitrogen adsorption measurements[a]

	Synthesis		SAXS		N_2 adsorpt.	
Silica	T (°C)	r (rpm)	R (nm)	s	a_{BET} (m^2 g^{-1})	a_{BET}/a_{geo}
Lys–Sil-1	60	1300	6.5	0.13	293	1.40
Lys–Sil-2	60	800	11.0	0.11	154	1.24
Lys–Sil-3	70	300	21.5	0.10	95	1.50
Ludox-TMA	—	—	13.4	0.13	115	1.13

[a] Polydispersity is expressed by the standard deviation from the mean particle size; a_{geo} is the geometric surface area.

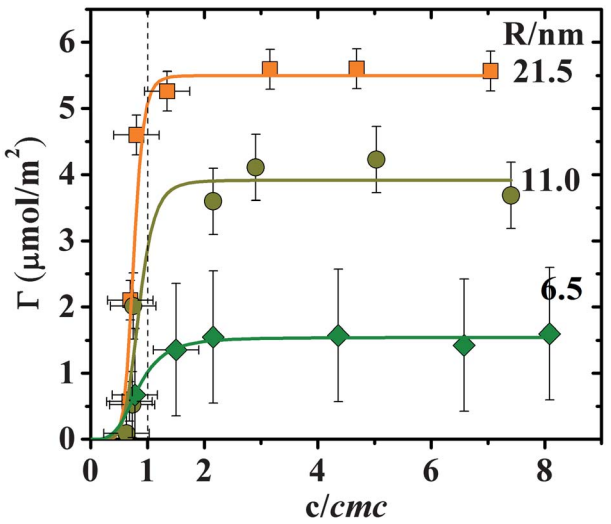

Fig. 2 Adsorption isotherms (20 °C) of the surfactant $C_{12}E_5$ at Lys–Sil silica particles of radius 6.5, 11 and 21.5 nm: experimental data and fits by the Gu–Zhu equation. The dashed vertical line indicates the cmc of the surfactant.

Table 2 Adsorption of $C_{12}E_5$ at Lys–Sil nanoparticles. Fit of adsorption data of Fig. 2 by eqn (1): maximum surface concentration Γ_m, adsorption constant K, nominal aggregation number of surface micelles n, and ratio of surface aggregation concentration to critical micelle concentration[a]

Silica	R (nm)	Γ_m (μmol m^{-2})	K	n	c_0/cmc
Lys–Sil-1	6.5	1.5	1.9	3.7	0.42
Lys–Sil-2	11	3.9	2.8	6.2	0.58
Lys–Sil-3	21.5	5.5	12	8.8	0.58

[a] cmc of $C_{12}E_5$ in water is found to be 7×10^{-5} M.

$$c_0/\mathrm{cmc} = \left(\frac{n-1}{n+1}\right)^{(n+1)/n} K^{-1/n} \qquad (2)$$

As indicated in Fig. 2, the uncertainty in the experimental values of Γ_m is large for the smallest particles. The uncertainty in c_0/cmc is estimated to ±20%.

The most interesting aspect of the adsorption isotherms in Fig. 2 is the strong decrease of the limiting surface concentration Γ_m with decreasing size of the Lys–Sil particles. In preliminary adsorption measurements for $C_{12}E_5$ on pure siliceous Ludox-TMA particles (R = 13.4 nm) we found a plateau value Γ_m = 4.5 mmol m^{-2}, which fits into the size dependence of Γ_m observed with the Lys–Sil particles.

Yokoi *et al.*[21] investigated the formation and properties of Lys–Sil nanoparticles using a combination of liquid-state ^{13}C NMR, solid-state ^{13}C CP/MAS NMR, thermogravimetry, and differential thermal analysis. They concluded that a substantial fraction of lysine used in the particle synthesis remains adsorbed at the nanospheres. To find out in what way adsorbed lysine may affect the adsorption of the surfactant we studied the adsorption of lysine onto pure siliceous nanoparticles.

2.3 Lysine adsorption onto silica nanoparticles

The adsorption of lysine was studied on a Ludox-TMA silica sol, as this material is free from any other organic base. The results are shown in Fig. 3. Within error limits the adsorption data can be represented by the Langmuir equation, $\Gamma^L = \Gamma^L_m bc/(1 + bc)$, where Γ^L is the surface concentration of lysine at equilibrium concentration c. We find a limiting surface concentration Γ^L_m = 1.8 μmol m^{-2} (corresponding to a surface density of 1.1 nm^{-2}), and adsorption constant b = 1.6 mM^{-1}. Our value of the limiting surface density is consistent with the value of 0.5 nm^{-2} reported by Yokoi *et al.*[21] for the specific conditions of their particle synthesis. From here on, the amount of lysine adsorbed at silica nanoparticles will be expressed by the relative surface concentration $\theta = \Gamma^L/\Gamma^L_m$ to avoid mix-up with the adsorption of the surfactant.

2.4 SANS study of surfactant aggregate structures

SANS measurements were made to study surfactant aggregate structures at silica nanoparticles in the absence and presence of lysine. As in the preceding studies,[14,15] SANS measurements were made with a H_2O–D_2O mixture that matches the scattering length density of the silica. In this contrast-match scenario the silica particles become invisible to the neutron beam. Hence in the absence of surfactant only a constant scattering background is observed, as shown in the inset in Fig. 4a. When a surfactant is added, a scattering intensity profile $I(q)$ appears which is characteristic of the shape and size of the surfactant aggregates and their arrangement in space. Fig. 4a shows the scattering profile for $C_{12}E_5$ in a 3.3 wt% Ludox-TMA silica dispersion at a surfactant concentration corresponding to Γ = 3.5 μmol m^{-2} (*i.e.*, well below the limiting adsorption, Γ_m = 4.5 μmol m^{-2}). Also shown in Fig. 4a is the scattering profile of the surfactant in the absence of silica, measured at a similar concentration but in pure D_2O, to enhance the scattering contrast. The scattering curve for $C_{12}E_5$ in the absence of silica can be represented quantitatively by the form factor model of wormlike micelles. The resulting fit parameters are given in Table 3.

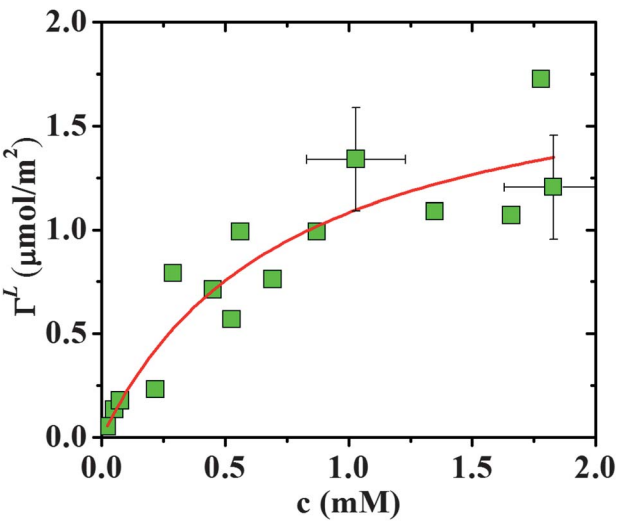

Fig. 3 Adsorption isotherm of lysine on Ludox-TMA silica: experimental data and fit by the Langmuir equation.

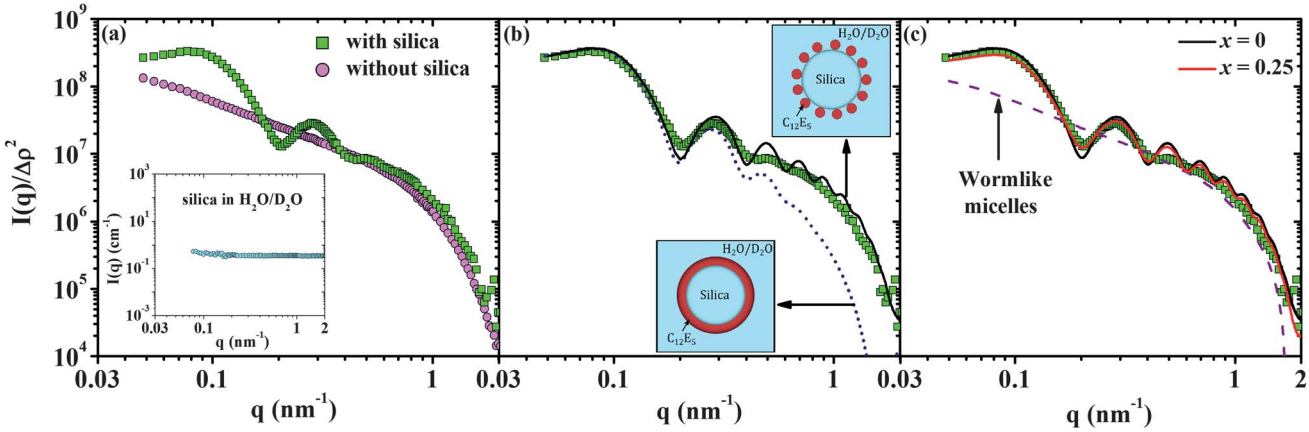

Fig. 4 SANS intensity profiles $I(q)$ for the surfactant $C_{12}E_5$ in a 3.3 wt% Ludox-TMA dispersion ($\Gamma = 3.5$ μmol m^{-2}) at silica/water contrast match conditions: (a) comparison of scattering profiles in the presence of silica particles (squares) and the corresponding amount of surfactant in the absence‡ of silica particles (circles) (the inset shows the contrast match of silica in absence of surfactant); (b) fit of the scattering curve by the shell model (dotted curve) and the micelle-decorated bead model (full curve), with $R_m = 2.2$ and $N = 105$; (c) fit to the scattering curve accounting for the dual population of the 25% surfactant as wormlike bulk micelles (red line) and rest adsorbed; the dashed curve in the graph is the form factor of the wormlike micelle.

Table 3 Analysis of SANS data for $C_{12}E_5$ adsorbed onto Ludox-TMA particles by the micelle-decorated bead model and spherical shell model[a]

	Γ (μmol m^{-2})	R_{bead} (nm)	R_m (nm)	$\Delta\rho$ ($\times 10^{-4}$ nm^{-2})	N_{mic}	L (nm)	x
Surf-micelles	3.5	13.37	2.2	2.36	105	—	0.25
Shell	3.5	13.37	—	2.36	—	4.0	—

[a] R_m is the radius of surface micelles and L is the thickness of shell according to core shell model.

The scattering profile of the surfactant in contact with silica particles was analysed in terms of two different models: (i) a spherical shell model,[12] assuming that the surfactant is forming a layer of uniform thickness L, and (ii) the micelle-decorated bead model,[22] assuming a random distribution of N spherical surface micelles of radius R_m located at a distance $R + R_m$ from the center of the silica particle. The parameters used to fit the data are given in Table 3. Fig. 4b shows that both models give a fair representation of the experimental data in the low-q regime including the local maximum near $q = 0.3$ nm^{-1}. For higher q the shell model predicts a steeper decrease of $I(q)$ than the observed scattering curve. This deviation indicates that the shell model underestimates the overall surface area of the surfactant aggregates. The micelle-decorated bead model gives a satisfactory fit of the entire scattering curve. The higher-order oscillations in the region of $q > 0.4$ nm^{-1} produced by this model are caused by artifacts arising from the Fourier transformation of the pair-correlation function of surface micelles to derive the inter-micellar structure factor. This pair-correlation function was generated by simulating random distributions of N spherical micelles on the silica bead (see ESI†). We stress that we have not attempted to determine the detailed shape of the surface micelles, but the model of spherical surface micelles was adopted for the sake of simplicity. However, we have tested if the fit can be further improved by assuming that a part of the surfactant is not adsorbed but exists in the form of free wormlike micelles. Specifically, the total scattering intensity was represented by

$$I(q) = (1 - x)I_{surf}(q) + xI_{bulk}(q) \quad (3)$$

where $I_{surf}(q)$ and $I_{bulk}(q)$ represent the scattering intensity functions of the micelle-decorated bead model and the model of free cylindrical micelles, respectively, and x is the fraction of scattering intensity contributed by the free micelles. Fig. 4c shows that eqn (3) with $x = 0.25$ gives indeed some improvement of the fit. However, more systematic studies and consideration of the finite experimental resolution of the SANS data (experimental smearing) would be necessary to discriminate between the small differences of the two models. The limitations of eqn (3) to account for the co-existence of two populations of surfactant micelles in the system are discussed below.

To establish the effect of lysine on the aggregate structure of the surfactant in the silica dispersion, SANS measurements were made for a set of samples of fixed concentration of $C_{12}E_5$ (20 mM) in 3.3 wt% dispersions of Ludox-TMA and with gradually increasing concentrations of lysine. From the known adsorption isotherm of lysine on Ludox-TMA (Fig. 3) its amount in the samples was adjusted such as to cover a wide range of surface concentrations while keeping the concentration of free lysine in the solution as low as possible ($c < 3$ mM). Scattering profiles for lysine surface concentrations θ from 0.004 to 0.76 are presented in Fig. 5a. It can be seen that the peak in $I(q)$ at $q \approx 0.3$ nm^{-1}, which is a measure of the amount of surfactant forming the adsorbed layer, decreases in height as the lysine concentration at the surface increases. A small peak is still detectable at a lysine surface concentration $\theta = 0.62$, but the peak has vanished

‡ The scattering curve for $C_{12}E_5$ without silica was measured in pure D_2O to enhance the contrast.

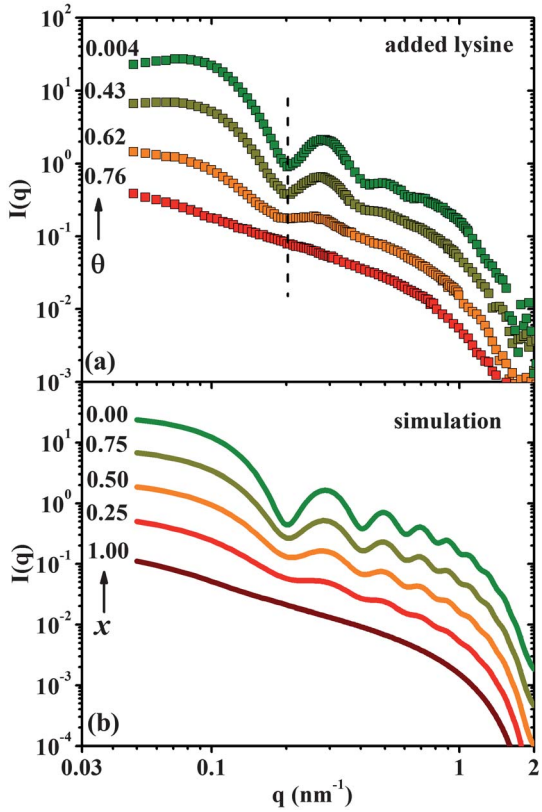

Fig. 5 (a) SANS experimental scattering curves for $C_{12}E_5$ in a 3.3 wt% dispersion of Ludox-TMA with increasing lysine concentration corresponding to relative surface concentrations θ from 0.004 to 0.76; (b) simulation of data in (a) based on eqn (3) with weight factor x of bulk micelles as given in the graph. In (a) and (b) curves for higher θ or x are shifted downward by factors of 3.

at $\theta = 0.76$. The scattering profile at this highest lysine concentration resembles the profile obtained for the surfactant in the absence of silica (*cf.* Fig. 4a). This clearly indicates that at $\theta > 0.75$ all surfactant has been displaced from the surface of the silica particles and is forming wormlike micelles in the aqueous phase. This conclusion is justified as it was confirmed by SANS measurements that lysine does not affect the scattering profile of $C_{12}E_5$ in the absence of the silica (not shown), and hence has no significant influence on the morphology of the bulk micellar aggregates at the lysine concentrations relevant in the present context. Quantitative modelling of the scattering profiles in terms of two co-existing populations of surfactant aggregates (surface micelles and bulk aggregates) in the presence of lysine was not practicable because too many of the relevant parameters were unknown. Instead, we checked if the gradual change of the scattering profile as a function of added lysine can be represented by eqn (3), *i.e.*, an incoherent superposition of contributions from surface micelles and free cylindrical micelles as in the bulk solution. Results for $x = 0$ (all surfactant forming spherical surface micelles), $x = 1$ (all surfactant forming wormlike micelles in solution) and intermediate states with $x = 0.25$, 0.5 and 0.75 are shown in Fig. 5b. The parameters used for simulating individual form factors of a silica bead with adsorbed surface micelles ($P_{\text{surf-mic}}(q)$) and free wormlike micelles in the bulk ($P_{\text{worm}}(q)$) are given in Table 4. It can be seen that the simulated curves reproduce the trends of the experimental scattering profiles as a function of θ (Fig. 5a).

Closer inspection of the SANS profiles in Fig. 5a reveals that the main oscillation in $I(q)$ shifts to lower values of q as the surface concentration θ of lysine increases. In terms of the simple core–shell model, this shift corresponds to an increase in the mean layer thickness from 4 nm to roughly 6 nm. This suggests that small surface concentrations of lysine are causing only partial detachment of the oxyethylene head groups of the surfactant, connected with a rehydration of these groups. Hence the lysine-induced weakening of the binding of surfactant to the surface may involve the formation of a water-rich layer between the surfactant aggregates and the surface, which ultimately leads to the complete detachment and reorganisation of the surfactant aggregates. This finding is reminiscent of the effect of temperature on the layer of $C_{12}E_5$ at silica particles as reported by Cummins *et al.*,[12] which was attributed to a temperature-induced reorganization and partial desorption of the surfactant.

3. Discussion

3.1 Size dependence of the adsorption of $C_{12}E_5$ on Lys–Sil

The sigmoidal shape of the adsorption isotherms in Fig. 2 is a well-known signature of aggregative adsorption of nonionic surfactants at hydrophilic surfaces.[6,9,11,20] On the other hand, the strong decrease of the maximum surface concentration of the surfactant with decreasing size of the Lys–Sil nanoparticles represents a remarkable new result. To our knowledge such a pronounced size effect on the adsorption has not been reported previously. This may be due to the difficulty of preparing oxide nanoparticles of well-defined size in this size range and determining the precise concentration of surfactant in the dispersion. Here we will discuss this finding from a point of view of the different structures of surfactant aggregates at the surface of the nanoparticles and in solution.

The SANS measurements presented in Section 2.4 have established that $C_{12}E_5$ is forming discrete surface aggregates at the Ludox-TMA silica particles, in agreement with our earlier findings with $C_{12}E_5$ at Stöber-type silica nanoparticles of similar size (16 nm).[14] In that paper we conjectured that surface micelles are preferred because the high surface curvature of small particles prevents an effective packing of surfactant molecules in a bilayer film. For a particle of radius R with an adsorbed bilayer film of thickness L the area at the midpoint plane of the bilayer exceeds the surface area of the particle by a factor $f = (1 + L/2R)^2$. For the present Lys–Sil particles and a bilayer thickness of 4 nm we have $f = 1.2$ for the largest particles ($R = 21.5$ nm), but $f = 1.7$ for the smallest particles ($R = 6.5$ nm). For large particles this curvature-induced handicap may be met by formation of an asymmetric bilayer, having a higher number of molecules in the outer layer. For the smallest particles, on the other hand, it appears that the curvature-induced handicap is too high for any form of bilayer structure. Instead, self-assembly apparently leads to discrete, more highly curved surface aggregates, as indicated by the SANS study. As shown above for $C_{12}E_5$ at Ludox-TMA particles, the data can be represented by spherical surface micelles of about 4.4 nm in diameter. Assuming that this also pertains to $C_{12}E_5$ adsorbed at the Lys–Sil particle, we

Table 4 Parameters used to simulate the form factors of spherical surface micelles and bulk wormlike micelles as further used in eqn (3)[a]

$P_{surf-mic}(q)$					$P_{worm}(q)$		
R_{bead} (nm)	s_{bead}	N_{mic}	R_m (nm)	s_{mic}	R_{worm} (nm)	L_c (nm)	L_k (nm)
13.37	0.13	100	2.2	0.1	2.0	142	40.5

[a] R_{bead} is the radius of the silica particle, s_{bead} its polydispersity, and s_{mic} is the polydispersity of the surface micelles, whereas R_{worm} is the radius, L_c and L_k are the contour and Kuhn length of wormlike bulk micelles.

may estimate the number of surface micelles per particle from the adsorption isotherms of the surfactant. The volume of adsorbed surfactant per particle at the plateau of the adsorption isotherm is given by $V_a = A\Gamma_m N_A v_a$, where $A = 4\pi R^2$ is the surface area of a particle of radius R, N_A is the Avogadro constant, and v_a is the volume of a surfactant molecule (v_a = 0.97 nm^3 for $C_{12}E_5$ hydrated with 10 water molecules[4]). The number of surface micelles per particle is then given by $N = V_a/v_m$, with $v_m = (4\pi/3)R_m^3$, where R_m is the radius of a surface micelle. The maximum number of micelles that can be accommodated at the particle surface can be estimated as $N_{max} = A'/a_m$, with $A' = 4\pi(R + R_m)^2$ and a_m the effective cross-sectional area of a surface micelle, which we approximate by $a_m = 4R_m^2$, assuming a square lattice. Values of N and N_{max} for surface micelles of radius $R_m = 2.2$ nm at the three Lys–Sil nanoparticles are given in Table 5. These values indicate that the fraction of surface occupied by adsorbed micelles is strongly increasing with the particle size. For the smallest particles (R = 6.5 nm), this estimate yields $N/N_{max} \approx 0.2$, *i.e.*, only a relatively small fraction of the surface is occupied with surface micelles. For the largest particles (R = 21.5 nm), on the other hand, our estimate yields $N/N_{max} > 1$, suggesting that at particles of this size the surfactant is not forming spherical surface micelles but aggregates which allow a higher packing density at the surface. This finding is plausible in view of the fact that $C_{12}E_5$ is forming flat (patchy) bilayer structures at planar surfaces.[6,7]

A particle-size induced transition from surface micelles to a surfactant bilayer can be rationalized by considering that adsorption of a surfactant bilayer onto a curved surface involves bending the bilayer and that the bending energy needed to wrap the particle can be balanced by the adhesion energy of the adsorbed layer. This is the essence of a phenomenological model by Lipowsky and Döbereiner,[23] which predicts a transition from the naked particle to the particle wrapped by the bilayer to occur at a critical particle radius $R_c = \sqrt{2\kappa/|w_{bi}|}$, where κ is the effective bending constant of the bilayer and w_{bi} is the adhesion energy per unit area. Small surface micelles may be adsorbed also onto particles of radius $R < R_c$, but due to the less effective packing their adhesion energy per unit area, w_{mic}, will be smaller than for an extended bilayer. On the basis of this argument we may expect a transition from a dense layer of micelles to a uniform bilayer to occur at a particle radius $R_{tr} = \sqrt{2\kappa/|w_{bi} - w_{mic}|}$. For surfactant bilayers we expect a bending constant $\kappa \approx 5kT$ and an attractive van der Waals interaction per unit area of the silica surface $w_{bi} \approx kT$. However, $|w_{bi} - w_{mic}|$ may be much smaller than w_{bi}. Assuming $|w_{bi} - w_{mic}| = 0.025kT$ leads to a transition at a radius R_{tr} = 20 nm, which is roughly the particle radius suggested by the analysis of the adsorption data (Table 5). Hence this model may explain the transition from discrete surface micelles to a uniform bilayer, but not the pronounced decrease of the number of surface micelles per unit area observed for the smaller particles. This size dependence of the surface concentration is considered in the following section.

Table 5 Adsorption of $C_{12}E_5$ onto Lys–Sil silica nanoparticles of radius R: measured maximum surface concentration Γ_m (Fig. 1), estimated number of spherical surface micelles (R_m = 2.2 nm) per silica particle, N, and N/N_{max}[a]

Silica	R (nm)	Γ_m (μmol m^{-2})	N	N/N_{max}
Lys–Sil-1	6.5	1.5	10	0.21
Lys–Sil-2	11.0	3.9	77	0.68
Lys–Sil-3	21.5	5.5	417	1.14

[a] Here N_{max} is the maximum number of surface micelles that can be accommodated at a particle of given radius (see text).

3.2 Effect of lysine on binding strength of surfactant

In order to gain some understanding of the low surface concentration of the surfactant at the smallest silica particles we need to look more closely at the anchoring of the surface micelles. For surfactants of the poly(oxyethylene)alkyl ether type, such as $C_{12}E_5$, on hydrophilic silica it is believed that hydrogen bonding of the silanol groups to the ether groups of the surfactant, either directly[24] or mediated by water molecules,[11] represents the dominant binding mechanism. To attain the necessary number of such bonds, surface micelles must acquire a sufficiently large contact area with the surface, which generally will imply some distortion of micellar shape relative to that in solution. For convex-shaped micelles the degree of distortion will depend on the mean curvature of the solid surface, being weakest at concave surfaces (as in nanopores)[25] and largest at spherical nanoparticles. Since the strain energy caused by distortion of the surface micelles is of opposite sign as the binding energy, surface micelle formation will become less favourable the higher the surface curvature of the particles. Accordingly, fewer surface micelles will be formed per unit area as the particle size decreases. Hence the concept of strained surface micelles may explain the observed decrease in the number of surface micelles with decreasing particle radius (Table 5).

The observed displacement of surfactant from the surface of the silica particles induced by adsorption of lysine may be rationalized on the basis of these arguments. Lysine is more strongly adsorbed onto the silica surface than the surfactant by hydrogen bonds between the weakly acidic silanol groups and the

basic terminal amino group of lysine. Accordingly, adsorption of lysine causes a decrease in the number density of free silanol groups at the silica particles and thus a weaker binding of the surface micelles. As can be seen in Fig. 5, the increase in the surface concentration θ of lysine (Fig. 5a) indeed correlates directly with the fraction x of the displaced surfactant (Fig. 5b).

Finally, we discuss the possible influence of lysine on the size dependence of the adsorption of $C_{12}E_5$ at the Lys–Sil nanoparticles (Fig. 2). Since the three samples of Lys–Sil were synthesized from the same reaction mixture, and particle size was tuned solely by the stirring rate and a weak temperature increase (see Table 1), we believe that the surface density of lysine and silanol groups was independent of particle size. This is in line with earlier published results on similar silica particles,[23] where the surface density of lysine on the Lys–Sil particles was estimated to be 0.5 nm^{-2}, and a value 3 nm^{-2} was adopted for the surface density of silanol groups as reported previously by Shenderovich *et al.*[26] From these values the fraction of silanol groups blocked by lysine was estimated to be 15%. This then implies that the surface density of free silanol groups at the Lys–Sil particles will be lower than for pure Stöber-type or Ludox-type silica. On the assumption that the binding strength of surface micelles of $C_{12}E_5$ is proportional to the surface density of free silanol, we may expect that the number of surface micelles on the Lys–Sil particles will be smaller than on Stöber-type or Ludox-type particles of equal size. Furthermore, we propose that this effect should be more pronounced for small, highly curved silica particles because in this case the straining energy would be higher than on larger particles. This conjecture is supported by the results of the earlier study of $C_{12}E_5$ at Stöber-type silica nanoparticles of radius 8 nm,[14] for which a significantly higher limiting surface concentration was found than on the present Lys–Sil particles of radius 11 nm. However, more systematic work is needed to corroborate this combined influence of particle size and density of binding sites.

3.3 Potential application relevance

The finding that a nonionic surfactant can be displaced readily from the surface of nanoparticles by small amounts of a more strongly adsorbed substance is of practical relevance for the formulation of dispersions stabilized by such surfactants. In addition, the displaced surfactant can cause significant changes in the macroscopic behaviour of the system. Since non-ionic surfactants like $C_{12}E_5$ are forming wormlike micelles in a wide temperature and concentration range their displacement from the surface can affect the rheological behaviour of the system.[27] For these surfactants it is even possible that the displacement of the surfactant drives the system from the one-phase region to the two-phase region of the surfactant + water phase diagram. For the present system this is demonstrated in Fig. 6. The phase diagram of the $C_{12}E_5$ + water exhibits a lower critical point (cloud point) at about 31 °C and 1 wt% surfactant.[28] Above this temperature the system separates into a water-rich and a surfactant-rich phase. Fig. 6a shows the turbidity *vs.* temperature of a 1 wt% Ludox-TMA dispersion containing 0.2 wt% $C_{12}E_5$, without and with added lysine. In the absence of lysine almost all surfactant is adsorbed at the particles (surface concentration $\Gamma =$ 4 μmol m^{-2}, *i.e.*, close to the limiting adsorption). The turbidity

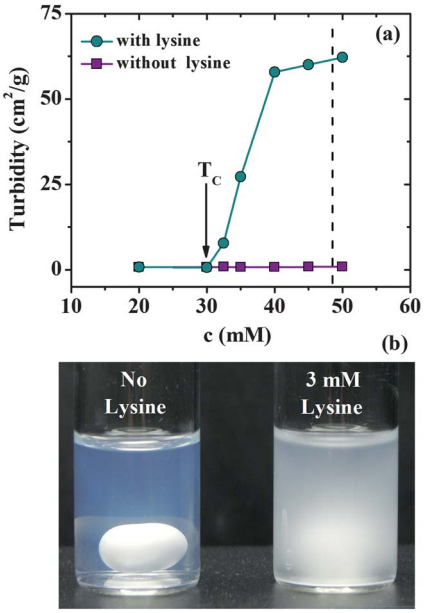

Fig. 6 (a) Turbidity of 5.2 mM $C_{12}E_5$ in a 1 wt% dispersion of Ludox-TMA without lysine (squares) and with 3 mM lysine (circles); (b) photograph of the two constantly stirred samples at a temperature well above the cloud point T_c (dashed line in (a)).

of this sample is moderately low and independent of temperature up to 50 °C. In the presence of lysine (3 mM), however, when the surfactant is detached from the particles, the turbidity of the stirred sample strongly increases at temperatures $T > T_c$, as most of the free surfactant is now forming droplets of the surfactant-rich phase. The silica particles remain dispersed in the aqueous phase. SAXS measurements on the samples without and with lysine show no increased intensity in the Guinier regime at different temperatures, confirming the absence of any aggregation of silica nanoparticles.[29] The scattering curves taken at temperatures from 20 to 50 °C superimpose (see ESI†). Photographs of the samples without and with lysine at a temperature above T_c are shown in Fig. 6b. This is a striking example to show the potential significance of such displacement effects for the formulation of nanoparticle dispersions with nonionic surfactants. Related phenomena were reported recently by Mustafina *et al.*[30]

4. Experimental

4.1 Materials

$C_{12}E_5$ (Sigma-Aldrich, ≥98%), 2,6-diaminohexanoic acid (lysine) (Fluka, purity >98%), tetraethyl orthosilicate (TEOS) (ABCR GmbH, purity >98%) and D_2O (Euriso-top, 99.9%) were used without further purification. Water was purified by a MilliPore QPAK®(2) unit. Ludox-TMA (30 wt% suspension in water) was supplied by Sigma-Aldrich and further purified by dialysis and filtration through 0.22 μm filters.

4.2 Synthesis of silica nanoparticles

Lys–Sil silica sols of different particle sizes were prepared by the hydrolysis of TEOS with water in the presence of the basic amino

acid lysine, as reported by Davis *et al.*[19] and Thomassen *et al.*[31] Particle size was tuned by using pre-optimized stirring rates and temperature conditions of the reaction mixture (Table 1). The resulting silica dispersions were dialyzed to remove unreacted TEOS, lysine and reaction byproduct ethanol. Details of the synthesis and product clean-up are given elsewhere.[29] The silica concentration of the resulting dispersions was determined gravimetrically (*ca.* 3 wt%).

The silica sols were characterized by small-angle X-ray scattering (SAXS), nitrogen adsorption, and transmission electron microscopy (TEM). SAXS measurements were performed on a SAXSess mc^2 instrument (Anton Paar, Austria) and the Saxsquant 3.50 software was used for data reduction and desmearing. Nitrogen adsorption isotherms at 77 K were determined on a Gemini III 2375 volumetric surface analyser (Micromeritics). For this purpose the dialysed silica dispersions were dried at 350 K for two days, then outgassed at 393 K for 1 h under vacuum, and finally reweighed to determine the precise mass of the sample. TEM images were taken by a FEI Technai G^2 20 S-Twin electron microscope operating at 200 kV.

4.3 Adsorption measurements

Adsorption isotherms of $C_{12}E_5$ on the silica sols were determined with dilute dispersions (0.1 wt%) by equilibration with appropriate amounts of the surfactant (24 h). After removal of the silica by centrifugation (4 h at 9500*g*) the concentration of non-adsorbed surfactant in the supernatant was determined by surface tension measurements. Surfactant concentrations above the cmc were determined by dilution with known amounts of water until the surface tension σ attained a value somewhat higher than σ_{cmc}. Systematic errors in the determination of the adsorbed amount in the plateau region of the adsorption isotherm can arise if not all the silica was removed by the centrifugation. In this case the surfactant can be desorbed from the particles in the dilution step, thus purporting a lower adsorption. Such an error will be largest for the smallest silica particles due to their slowest sedimentation in the centrifugation step. Systematic errors in the surface concentration Γ of adsorbed surfactant can also arise from errors in the silica concentration of the dispersion (up to $\pm$5%) and the specific surface area of the silica ($\pm$2%).

The extent of lysine binding at the silica surface was determined by adsorption measurements on Ludox-TMA. Lysine solutions of appropriate concentrations in water were prepared and a fixed volume of the silica dispersion was added. After equilibration (24 h) the silica sol was separated from the supernatant by centrifugation (2 h at 21 000*g*) and the residual concentration of lysine was determined by reaction with ninhydrin to Ruhman's purple which was detected by its absorbance at 570 nm.

4.4 SANS measurements

Dispersions of Ludox-TMA (3.3 wt%) were prepared in a H_2O–D_2O mixture with 61.7 wt% D_2O, which has the same scattering length density (SLD) as silica (SLD = 3.54×10^{-4} nm^{-2}). A constant amount of $C_{12}E_5$ but increasing quantities of lysine were added to these silica dispersions. SANS measurements were carried out using the SANS-II instrument at the Paul Scherrer Institute, Villigen (CH). Three different sample-to-detector distances were used to cover values of the scattering vector q from 0.05 to 2.8 nm^{-1}. The 2D scattering data were reduced to 1D profiles using the *BerSANS* software package. *SciLab* was used for building up codes of different models for further analysis of the scattering curves.

5. Conclusions

This study has shown that the self-assembly of surfactants in a dispersion of nanoparticles can be tuned by an additive which modifies the surface energy by adsorption onto the particles. Lysine acts as an effective surface modifier in the present system. Small concentrations of lysine cause a complete displacement of the surfactant $C_{12}E_5$ from silica particles. SANS measurements reveal that the displacement process represents a morphological transition from discrete surface micelles attached to the particles to elongated (wormlike) micelles in the aqueous bulk phase. The detachment seems to proceed *via* an intermediate state in which a hydrated layer of adsorbed lysine intercalates between the surfactant aggregates and the surface. Further SANS studies are needed to elucidate this process.

For Lys–Sil particles we find a pronounced decrease of the maximum surface concentration of the surfactant with decreasing particle size. Our study suggests that this size effect is caused by the adsorbed layer of lysine, which reduces the binding strength of the surfactant head groups, in combination with the increasing curvature of the solid surface. For the smallest particles (diameter 13 nm) only a fraction of their surface is decorated with surface micelles. We speculate that this may be a consequence of a stronger distortion of surface micelles that is needed for attaining a sufficiently large contact area with the surface of small particles when some of the sites are blocked by lysine. The much higher limiting adsorption of the surfactant at the largest particles (43 nm) indicates that in this case the surfactant is not forming discrete surface micelles but less highly curved aggregates which allow a higher packing density at the surface. We present a simple model to account for such a transition in surface aggregate structure. Hence, this study can contribute to a better understanding of the factors controlling the self-assembly of surfactants at nanoparticles. This will be useful in the formulation of nanoparticle dispersions and their application in particle nanotechnology.

Acknowledgements

We wish to thank Dr D. M. Lugo and Dr S. Prevost for their support in the data analysis and interpretation, and S. Selve (ZELMI, TU Berlin) for help with TEM measurements. This work is based on experiments performed at the Swiss spallation neutron source SINQ, Paul Scherrer Institute, Villigen, Switzerland, and has been supported by the European Commission under the 7th Framework Programme through the 'Research Infrastructures' action of the 'Capacities' Programme, contract no: CP-CSA_INFRA-2008-1.1.1 number 226507-NMI3. Financial support by the German Research Foundation (DFG) in the framework of IGRTG 1524 is also gratefully acknowledged.

Notes and references

1 *Handbook of Applied Surface and Colloid Chemistry*, ed. K. Holmberg, D. O. Shah and M. J. Schwuger, John Wiley, New York, 2002; S. Paria and K. C. Khilar, *J. Colloid Interface Sci.*, 2004, **110**, 75; L. K. Limbach, R. Bereiter, E. Müller, R. Krebs, R. Gälli and W. J. Stark, *Environ. Sci. Technol.*, 2008, **42**, 5828; N. Veronovoski, P. Andeozzi, C. L. Mesa, M. S. Smol and V. Ribitsch, *Colloid Polym. Sci.*, 2010, **288**, 387; R. Zhang and P. Somasundaran, *Adv. Colloid Interface Sci.*, 2006, **123–126**, 213.

2 N. A. Klimenko and A. M. Koganovskii, *Kolloidn. Zh.*, 1974, **36**, 151; N. A. Klimenko, V. L. Kofanov and E. G. Sivalov, *Kolloidn. Zh.*, 1981, **43**, 287.

3 P. Levitz, *Langmuir*, 1991, **7**, 1595.

4 M. R. Böhmer, L. K. Koopal, R. Janssen, E. M. Lee, R. K. Thomas and A. R. Rennie, *Langmuir*, 1992, **8**, 2228.

5 S. Manne and H. E. Gaub, *Science*, 1995, **270**, 1480.

6 F. Tiberg, *J. Chem. Soc., Faraday Trans.*, 1996, **92**, 531.

7 L. M. Grant, F. Tiberg and W. A. Ducker, *J. Phys. Chem. B*, 1998, **102**, 4288.

8 R. Steitz, P. Müller-Buschbaum, S. Schemmel, R. Cubitt and G. H. Findenegg, *Europhys. Lett.*, 2004, **67**, 962.

9 O. Dietsch, A. Eltekov, H. Bock, K. E. Gubbins and G. H. Findenegg, *J. Phys. Chem. C*, 2007, **111**, 16045.

10 J. Penfold, E. Staples and I. Tucker, *Langmuir*, 2002, **18**, 2967.

11 M. K. Matsson, B. Kronberg and P. M. Claesson, *Langmuir*, 2004, **20**, 4051.

12 P. G. Cummins, J. Penfold and E. Staples, *J. Phys. Chem.*, 1992, **96**, 8092.

13 J. Penfold, E. Staples, I. Tucker and P. Cummins, *J. Phys. Chem.*, 1996, **100**, 18133.

14 D. M. Lugo, J. Oberdisse, M. Karg, R. Schweins and G. H. Findenegg, *Soft Matter*, 2009, **5**, 2928.

15 D. M. Lugo, J. Oberdisse, A. Lapp and G. H. Findenegg, *J. Phys. Chem. B*, 2010, **114**, 4183.

16 K. P. Sharma, V. K. Aswal and G. Kumaraswami, *J. Phys. Chem. B*, 2010, **114**, 10986.

17 S. Kumar and V. K. Aswal, *J. Phys.: Condens. Matter*, 2011, **23**, 035101.

18 S. Ahualli, G. R. Iglesias, W. Wachter, M. Dulle, D. Minami and O. Glatter, *Langmuir*, 2011, **27**, 9182.

19 T. M. Davis, M. A. Snyder, J. E. Krohn and M. Tsapatsis, *Chem. Mater.*, 2006, **18**, 5814.

20 T. Gu and B.-Y. Zhu, *Colloids Surf.*, 1990, **44**, 81; B.-Y. Zhu, T. Gu and X. Zhao, *J. Chem. Soc., Faraday Trans. 1*, 1989, **85**, 3819.

21 T. Yokoi, J. Wakabayashi, Y. Otsuka, W. Fan, M. Iwama, R. Watanabe, K. Aramaki, A. Shimojima, T. Tatsumi and T. Okubo, *Chem. Mater.*, 2009, **21**, 3719.

22 G. Despert and J. Oberdisse, *Langmuir*, 2003, **19**, 7604; J. Oberdisse, *Phys. Chem. Chem. Phys.*, 2004, **6**, 1557.

23 R. Lipowsky and H.-G. Döbereiner, *Europhys. Lett.*, 1998, **43**, 219.

24 S. Partyka, S. Zaini, M. Lindeheimer and B. Brun, *Colloids Surf.*, 1984, **12**, 255; P. Trens and R. Denoyel, *Langmuir*, 1993, **9**, 519.

25 D. Müter, T. Shin, B. Demé, P. Fratzl, O. Paris and G. H. Findenegg, *J. Phys. Chem. Lett.*, 2010, **1**, 1442.

26 I. G. Shenderovich, D. Mauder, D. Akcakayiran, G. Buntkowsky, H.-H. Limbach and G. H. Findenegg, *J. Phys. Chem. B*, 2007, **111**, 12088.

27 R. Strey, *Ber. Bunsenges. Phys. Chem.*, 1996, **100**, 182.

28 R. Strey, R. Schomäcker, D. Roux, F. Nallet and U. Olsson, *J. Chem. Soc., Faraday Trans.*, 1990, **86**, 2253.

29 B. Bharti, J. Meissner and G. H. Findenegg, *Langmuir*, 2011, **27**, 9823.

30 A. R. Mustafina, J. G. Elistratova, O. D. Bochkova, V. A. Burilov, S. V. Fedorenko, A. I. Konovalov and S. Y. Soloveva, *J. Colloid Interface Sci.*, 2011, **354**, 644.

31 L. C. J. Thomassen, A. Aerts, V. Rabolli, D. Lison, L. Gonzalez, M. Kirsch-Volders, D. Napierska, P. H. Hoet, C. E. A. Kirschhock and J. A. Martens, *Langmuir*, 2010, **26**, 328.

Addition and correction

Note from RSC Publishing

This article was originally published with incorrect page numbers. This is the corrected, final version.

The Royal Society of Chemistry apologises for these errors and any consequent inconvenience to authors and readers.